Stanford Geothermal Program
Interdisciplinary Research in
Engineering and Earth Sciences
STANFORD UNIVERSITY
Stanford, California

SGP-TR-62

TEMPERATURE TRANSFER IN A CONVECTION-DOMINANT, NATURALLY FRACTURED GEOTHERMAL RESERVOIR UNDERGOING FLUID INJECTION

By

John Duncan Gage Moody

June 1982

Financial support was provided through the Stanford Geothermal Program under Department of Energy Contract No. DE-AT03-80SF11459 and by the Department-of Petroleum Engineering, Stanford University.

TABLE OF CONTENTS

ABSTRACT

This study considers the heat and fluid flow characteristics of an infinite, naturally fractured geothermal reservoir in which forced convection is the only form of heat transfer. For simplicity, it is assumed that there is only one injector well and no producer wells in the system. Further, primary porosity is neglected and the fracture porosity is assumed to be constant throughout the reservoir.

With these specifications, the governing equations are derived from an energy balance, and solved using dimensionless parameters and the Laplace transform. Both numerical inversion and analytical inversion are then used, though only the latter appears to give a reliable solution. The results are plotted as dimensionless temperature versus dimensionless volume swept (called dimensionless radius), and the velocity of the thermal front in the rock and water determined.

1. INTRODUCTION

Owing to the analogous nature of many petroleum and geothermal reservoir phenomena, studies of naturally fractured petroleum reservoirs are often of great value in the study of geothermal systems. This effort draws upon one such study by Warren and Root(1962)[1], and a later paper by Mavor(1978)[2], which present analytical flow models for the analysis of pressure-production response. A somewhat similar flow problem for geothermal reservoirs is presented in this report, in order to examine the heat transfer during cold water injection.

The focus of this study is to determine the location of the thermal front in the reservoir, as well as examine its form and behaviour. These results should then yield the velocity of the thermal front, in both the rock and water, relative to that of the injected fluid. While their validity is limited by certain simplifying assumptions, the results should also represent a useful step toward solving related problems of greater complexity.

2. ASSUMPTIONS

1. Single well in an infinite reservoir, radial flow.

   This paper considers only the case of one injector well in an infinite system. Superposition is therefore not used.

2. Steady state flow of injected fluid.

   The solution to this problem will not be valid for short times during which transient fluid flow occurs.

3. Only convection heat transfer, conduction not considered.

   Conduction of heat in the reservoir rock is assumed to be small compared to forced convection. This assumption should be good for all but very long time.

4. Initial reservoir temperature the same throughout system.

5. Only secondary or fracture porosity

   The effects of primary porosity are not considered in this study. It is assumed that this porosity is small enough to be neglected or that the model must be adjusted to account for its effect on the transfer of heat and fluid flow in the reservoir.

6. Reservoir uniformly fractured and fracture width constant.

This problem does not consider significant variation in fracture width anywhere in the reservoir. Vertically, fracture length is limited by the height of the producing interval. Orientation of the fracture need not be specified as it is implicit in the effective porosity.

7. Effective porosity constant throughout reservoir.

In order that convection heat transfer occur, the reservoir rock must be swept by the injected fluid. the effective porosity constraint requires that each fracture be oriented such that it conducts the injected fluid radially. Concentric and other fractures orthogonal to the direction of flow are not included in this porosity. The fracture porosity used for this model therefore is less that the total fracture porosity of the system. Figure 1 presents an element volume of such a reservoir, in which neither the degree of fracturing nor the fracture width changes.

All of the above constraints are introduced so as to keep the reservoir flow model simple but at the same time still realistic.

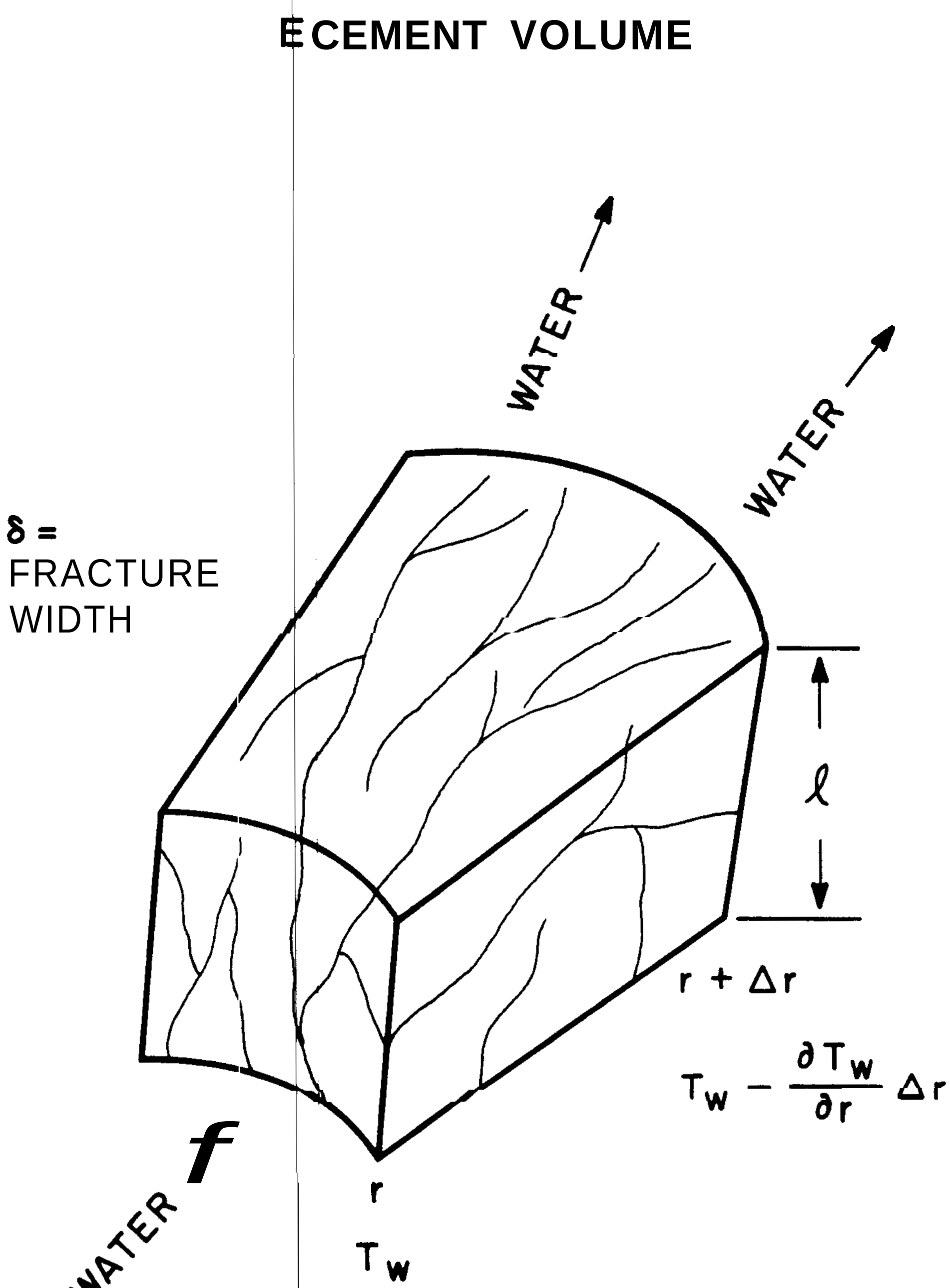
ECEMENT VOLUME
WATER
WATER
δ = FRACTURE WIDTH
ℓ
r + Δr
$T_w - \frac{\partial T_w}{\partial r} \Delta r$
WATER
r
T_w

FIG. 1

3. ENERGY BALANCE

An element volume of the naturally fractured reservoir is shown is Fig. 1. An energy balance on this element yields the following two equations:

$$\text{(i)} \qquad -\rho_w q_w C_{vw}\left\{\left(T_w + \frac{\partial T_w}{\partial r}\Delta r\right) - T_w\right\} - h_c A_{Rw}(T_w - T_R) = \rho_w C_{vw} V_w \frac{\partial T_w}{\partial t}$$

$$\text{(ii)} \qquad h_c A_{Rw}(T_w - T_R) = \rho_R C_{vR} V_R \frac{\partial T_R}{\partial r}$$

(The symbols used are defined in APPENDIX 1 : Nomenclature and Typical Values)

Note that while the rock and water volumes of the element are different, they share the same surface area and have identical convection terms. Their combined volumes give the total element volume. In addition, the water volume and surface area is equal to the fracture volume and surface area of the element. Finally, note that the storage term in (i) is negative.

Temperature in this reservoir is a function of the distance from the injection well and the time since the start of injection. Given any particular radius and time, the solution of these two equations will give both the rock and water temperature.

Rewriting the above equations with their appropriate initial conditions and boundary conditions,

$$-\rho_w q_w C_{vw} \frac{\partial T_w}{\partial r} - h_c A_{Rw}(T_w - T_R) = \rho_w C_{vw} V_w \frac{\partial T_w}{\partial t} \tag{1}$$

$$h_c A_{Rw}(T_w - T_R) = \rho_R C_{vR} V_R \frac{\partial T_R}{\partial t} \tag{2}$$

$$\text{Intial Conditions : } T_w(r,0) = T_R(r,0) = T_{wi} \tag{3a}$$

$$\text{Boundary Condition : } T_w(r_w,t) = T_{inj} \tag{3b}$$

The total volume of the element is given by :

$$V_e = 2\pi r \Delta r \ell \tag{4}$$

While for assumptions 5, 6, and 7 of section 2 to hold, the water and rock element volumes also must be given by :

$$V_w = \Phi_2 V_e \quad (4c) \qquad V_R = (1 - \Phi_2) V_e \quad (4b)$$

Alternatively, the total volume can be expressed as :

$$V_e = V_W + V_R \tag{5}$$

And the rock surface area for heat exchange can be written as :

$$A_{Rw} = \frac{2V_w}{\delta} \tag{6}$$

Where : Φ_2 = fracture porosity

δ = fracture width

Using equation (5), and substituting (4), and (6) into equations (1) and (2) yields,

$$-\frac{B}{r}\frac{\partial T_w}{\partial r} - D(T_w - T_R) = M_w \frac{\partial T_w}{\partial t} \tag{7}$$

$$D(T_w - T_R) = M_R \frac{\partial T_R}{\partial t} \tag{8}$$

Where the new constants are defined as :

$$B = \frac{\rho_w q_w C_{vw}}{2\pi \ell} \qquad D = \frac{2h_c \Phi_2}{\delta} \tag{8b}$$

$$M_w = \rho_w C_{vw} \Phi_2 \qquad M_R = \rho_R C_{vR}(1 - \Phi_2) \tag{8c}$$

4. DIMENSIONLESS FORM OF EQUATIONS

Before solving equations (7) and (8) for $T_w(r,t)$ and $T_R(r,t)$, it is convenient to re-state these equations using dimensionless parameters :

Dimensionless Time.

$$t_D = \frac{Dt}{M_R} \qquad \text{or} \qquad t_D = \frac{2h_c\Phi_2 t}{\rho_R C_{vR}(1-\Phi_2)\,\delta} \tag{9a}$$

Dimensionless radius,

$$r_D = \frac{D(r^2 - r_w^2)}{2B} \qquad \text{or} \qquad r_D = \frac{2\pi\ell(r^2 - r_w^2)\,h_c\Phi_2}{\rho_w C_{vw} q_w} \tag{9b}$$

Dimensionless temperature,

$$T_w = \frac{T_w - T_{wi}}{T_{inj} - T_{wi}} \qquad \text{and} \qquad T_R = \frac{T_R - T_{wi}}{T_{inj} - T_{wi}} \tag{9c}$$

Note that the dimensionless radius term is actually dimensionless volume and must not be confused with the r/rw used in pressure-production problems.

Re-stated in dimensionless form, equations (7) and (8) become :

$$-\frac{\partial T_w}{\partial r_D} - (T_w - T_R) = \frac{M_w}{M_R}\frac{\partial T_w}{\partial t_D} \qquad (10)$$

$$(T_w - T_R) = \frac{\partial T_R}{\partial t_D} \qquad (11)$$

Initial Condition : $T_w(r_D, 0) = T_R(r_D, 0) = 0$ (12a)

Boundary Condition : $T_w(0, t_D) = 1$ (12b)

5. SOLUTION BY THE LAPLACE TRANSFORM

Using the Laplace transform, equations (10) and (11) are transformed in time and solved simultaneously in Laplace space to produce an ordinary differential equation in terms of $\overline{T}_W(r_D,S)$, where S is the Laplace transformed variable. This equation is solved using the boundary condition and $\overline{T}_R(r_D,S)$ is then easily determined. The details of this procedure are given in Appendix B.

The solutions are found to be :

$$\overline{T}_W(r_D,S) = \frac{1}{S}\,\mathrm{Exp}\left\{ -r_D\left(1 + \frac{M_W}{M_R}S - \frac{1}{S+1} \right) \right\} \tag{13a}$$

$$\overline{T}_R(r_D,S) = \frac{1}{S(S+1)}\,\mathrm{Exp}\left\{ -r_D\left(1 + \frac{M_W}{M_R}S - \frac{1}{S+1} \right) \right\} \tag{13b}$$

The asymptotic forms of equations (13a) and (13b) are given in Appendix 3.

6. INVERSION OF LAPLACE SOLUTIONS

It is now possible to invert both equations (13a) and (13b) and arrive at an analytical solution to the problem. While it was necessary to first determine the water temperature solution (13b) using the boundary condition, the order of inversion makes no difference.

Inversion of Equation for Rock Temperature, $\overline{T}_R(r_D, S)$:

Re-writing equation (13b) in a more convenient order for inverting,

$$\overline{T}_R(r_D,S) = \mathrm{Exp}(-r_D)\ \mathrm{Exp}(-r_D \frac{M_W}{M_R} S)\ \frac{1}{S}\ \frac{1}{S+1}\ \mathrm{Exp}(\frac{r_D}{S+1}) \qquad (14)$$

Step #1

Applying the shifting theorem;

$$T_R(r_D,t_D^*) = u(t_D^*)\ \mathrm{Exp}(-r_D)\ \pounds^{-1}\{ \frac{1}{S}\ \frac{1}{S+1}\ \mathrm{Exp}(\frac{r_D}{S+1}) \} \qquad (15)$$

where,

$$t_D^* = (t_D - \frac{M_W}{M_R} r_D) \qquad (15a)$$

and $u(t_D^*)$ is the step unction :

$$u(t_D^*) = 0 \quad t_D^* < 0 \qquad \text{an} \qquad u(t_D^*) = 1 \quad t_D^* \geq 0 \tag{15b}$$

Application of the convolution theorem gives,

$$T_R(r_D,t_D^*) = u(t_D^*) \, Exp(-r_D) \, f_1(t_D^*) * f_2(t_D^*) \tag{16}$$

Where,

$$f_1(t_D^*) * f_2(t_D^*) = \int_0^{t_D^*} f_1(t_D^*) \, f_2(t_D^* - \tau) \, \partial\tau \tag{16a}$$

Step #2

Equation (16) is reduce further using the following relations:[3]

$$F_1(S) = \frac{1}{S} \tag{17}$$

$$F_2(S) = F(S+1) = \frac{1}{S+1} \, xp(\frac{r_D}{S+1}) \tag{17.1}$$

Inverting,

$$\mathcal{L}^{-1}\{ F_1(S) \} = \mathcal{L}^{-1}\{ \quad \} = 1 \tag{17.2}$$

And,

$$\mathcal{L}^{-1}\{ F (S + 1) \} = Exp(- t_D^*)\ \mathcal{L}^{-1}\{ F (S) \} \tag{17.3}$$

Where,

$$\mathcal{L}^{-1}\{ F (S) \} = \mathcal{L}^{-1}\{ \quad Exp(\frac{r_D}{S}) \} \tag{17.4}$$

From Abramowitz and Stegun [4], the inverse of equation (17.4) is found to be :

$$\mathcal{L}^{-1}\{ \frac{1}{s} Exp(\frac{A}{s}) \} = I_0(2 \sqrt{A t}) \tag{17.5}$$

and if,

$$V = (t_D^* - \tau) \quad , \qquad A = r_D \tag{17.6}$$

then the rock temperature solution becomes :

$$T_R(r_D,t_D) = u (t_D^*) Exp(-r_D) \int_0^{t_D^*} Exp(-V)\ I_0(2 \sqrt{r_D V})\ \partial V \tag{18}$$

Step #3

Although the integral in equation (18) is not easily found in many tables of integrals, an excellent discussion of it appears in Luke, 'Integrals of Bessel Functions'[5]. This book also contains some valuable references for further investigation. After some rearranging, the integral is :

$$\int_0^x \mathrm{Exp}(-V)\ I_0(\ 2\sqrt{y\ V}\ )\ \partial V = \mathrm{Exp}(y)\ \{\ 1 - J(x,y)\ \} \qquad (19)$$

where J(x,y), a function defined in terms of the above integral, is expanded below.

If we let,

$$y = r_D \quad , \qquad x = t_D^* \qquad \begin{matrix}(19.1)\\(A4.1)\end{matrix}$$

the rock and water temperature (from appendix 4) then become :

$$T_R(r_D,t_D^*) = u(\ t_D^*)\ \{\ 1 - J(\ t_D^*,r_D)\ \} \qquad (19.2)$$

$$T_w(r_D,t_D) = u(\ t_D^*)\ \mathrm{Exp}\ \{\ -(\ r_D + t_D^*)\ \}\ I_0(\ 2\sqrt{r_D\ t_D^*}\ ) + T_R(r_D,t_D^*)$$

(19.3), (A4.4)

This analytical solution is checked for the initial and boundary values, as well as the asymptotic forms in Appendix 3.

The expansion of the function J(x,y) has two different forms :[6]

Case #1

$\sqrt{\frac{y}{x}} < 1$:

$$J(x,y) = \mathrm{Exp}\left\{ -(x+y) \right\} \sum_{k=0}^{\infty} \sqrt{\frac{y}{x}}^{\,k} I_k(2\sqrt{xy}) \tag{20}$$

Case #2

$\sqrt{\frac{y}{x}} > 1$:

$$J(x,y) = 1 - \mathrm{Exp}\left\{ -(x+y) \right\} \sum_{k=1}^{\infty} \sqrt{\frac{y}{x}}^{\,-k} I_k(2\sqrt{xy}) \tag{21}$$

At this point in the derivation, the reader is referred to Appendix 4, where both the rock and water temperature expansions are derived in greater detail.

From Appendix 4, the analytical results are :

Case #1

$$\sqrt{\frac{r_D}{t_D^*}} \leq 1 \quad :$$

Rock Temperature :

$$T_R(r_D,t_D^*) = u\,(t_D^*)\left(1 - \mathrm{Exp}\left\{-\,(r_D + t_D^*)\right\}\sum_{k=0}^{\infty}\left(\sqrt{\frac{r_D}{t_D^*}}\right)^{k} I_k\left(2\sqrt{r_D\,t_D^*}\,\right)\right) \tag{22}$$

Water Temperature :

$$T_w(r_D,\,t_D^*) = u(t_D^*)\left(1 - \mathrm{Exp}\left\{-\,(r_D + t_D^*)\right\}\sum_{k=1}^{\infty}\left(\sqrt{\frac{r_D}{t_D^*}}\right)^{k} I_k\left(2\sqrt{r_D\,t_D^*}\right)\right) \tag{23}$$

Case #2

$$\sqrt{\frac{r_D}{t_D^*}} \geq 1$$

Rock Temperature :

$$T_R(r_D,\ t_D^*) = u(\ t_D^*\ )\ \mathrm{Exp}\left\{ -\ (\ r_D + t_D^*) \right\} \sum_{k=1}^{\infty} \left(\sqrt{\frac{r_D}{t_D^*}}\right)^{-k} I_k(\ 2\sqrt{r_D\ t_D^*}\ ) \tag{24}$$

Water Temperature :

$$T_w(r_D,\ t_D^*) = u(\ t_D^*\ )\ \mathrm{Exp}\left\{ -\ (\ r_D + t_D^*) \right\} \sum_{k=0}^{\infty} \left(\sqrt{\frac{r_D}{t_D^*}}\right)^{-k} I_k(\ 2\sqrt{r_D\ t_D^*}\ ) \tag{25}$$

In both of the above cases, the convection term has the form :

$$T_w(r_D,t_D^*) - T_R(r_D,t_D) = u(t_D - \frac{M_w}{M_R}\ r_D)\ \mathrm{Exp}\left\{ -\ (\ r_D + t_D^*) \right\} I_0(\ 2\sqrt{r_D\ t_D^*}\ ) \tag{26}$$

The above expansions are also checked at the initial and boundary values, as well as the limiting forms, in Appendix 3.

7. NUMERICAL EVALUATION OF ANALYTICAL RESULT

The expansions for both cases described can be evaluated numerically using the following approximations for the given modified Bessel functions [7].

For small values of x

$$I_\nu(x) = \frac{\left(\frac{1}{2}x\right)^\nu}{\Gamma(\nu+1)} , \qquad \nu = 0, 1, 2, \ldots \tag{27a}$$

For large values of x

$$I_\nu(x) = \frac{\operatorname{Exp}(x)}{\sqrt{2\pi x}} \left\{ 1 - \frac{4\nu^2-1}{8x} + \frac{(4\nu^2-1)(4\nu^2-9)}{2!(8x)^2} - \frac{(4\nu^2-1)(4\nu^2-9)(4\nu^2-25)}{3!(8x)^3} \right.$$

$$+ \ldots\ldots \tag{27b}$$

or more simply,

$$I_\nu(x) = \frac{\operatorname{Exp}(x)}{\sqrt{2\pi x}} f(\nu, x) \tag{28}$$

Since the dimensionless terms for radius and time are large for almost all times, the approximation for large values is used in expanding the solutions.

If we let,

$$\alpha = 2\sqrt{r_D t_D^*} \qquad (27) \qquad\qquad \beta = (r_D + t_D^*) \qquad (28)$$

the solutions become :

Case #1

$$T_R(r_D,t_D^*) = u(t_D^*)\left(1 - \frac{\mathrm{Exp}(\alpha - \beta)}{\sqrt{2\pi\alpha}} \sum_{k=0}^{\infty} \sqrt{\frac{r_D}{t_D^*}}^{\,k} f(k,x)\right) \qquad (30)$$

$$T_w(r_D,t_D^*) = u(t_D^*)\left(1 - \frac{\mathrm{Exp}(\alpha - \beta)}{\sqrt{2\pi\alpha}} \sum_{k=1}^{\infty} \sqrt{\frac{r_D}{t_D^*}}^{\,K} f(k,x)\right) \qquad (31)$$

Case 82

$$T_R(r_D,t_D^*) = u(t_D^*) \frac{\mathrm{Exp}(\alpha - \beta)}{\sqrt{2\pi\alpha}} \sum_{k=1}^{\infty} \sqrt{\frac{r_D}{t_D^*}}^{\,-k} f(k,x) \qquad (32)$$

$$T_w(r_D,t_D^*) = u(t_D^*) \frac{\mathrm{Ex{\sim}}((\alpha - \beta)}{\sqrt{2\pi\alpha}} \sum_{k=0}^{\infty} \sqrt{\frac{r_D}{t_D^*}}^{\,-k} f(k,x) \qquad (33)$$

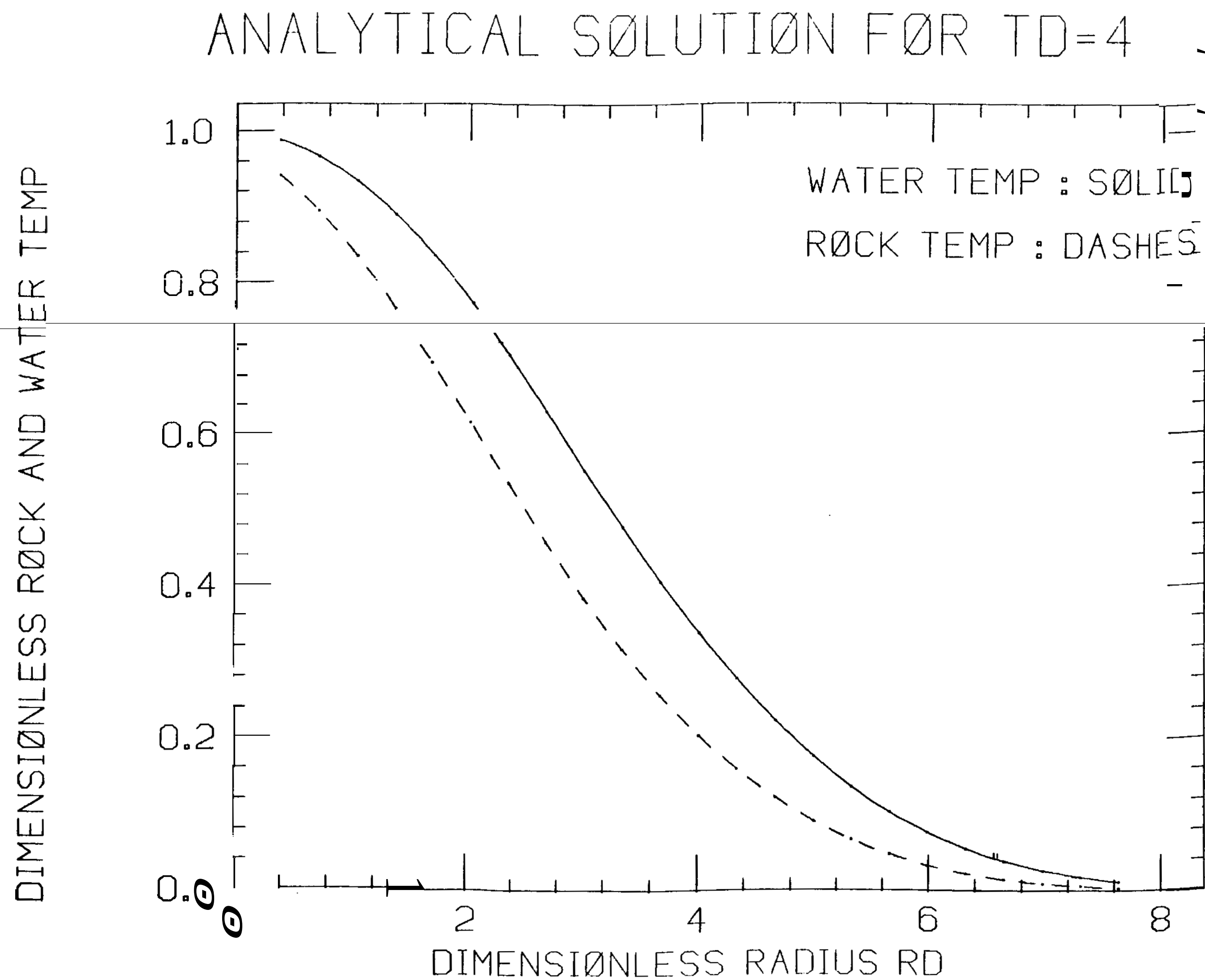
ANALYTICAL SØLUTIØN FØR TD=4
WATER TEMP : SØLID
RØCK TEMP : DASHES
DIMENSIØNLESS RØCK AND WATER TEMP
0.0
0.2
0.4
0.6
0.8
1.0
2
4
6
8
DIMENSIØNLESS RADIUS RD

FIG. 2

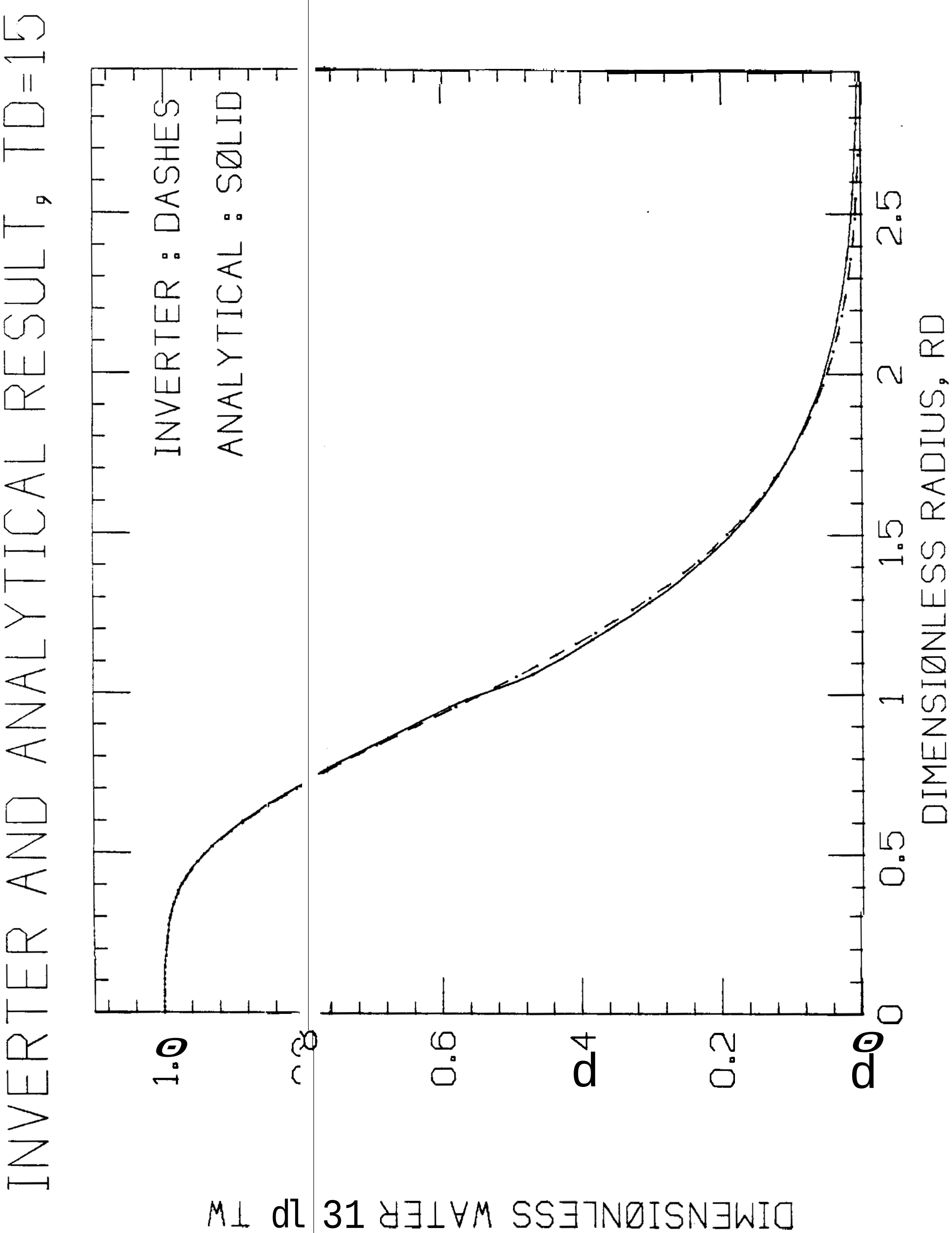

INVERTER AND ANALYTICAL RESULT, TD=15
INVERTER : DASHES
ANALYTICAL : SØLID
DIMENSIØNLESS RADIUS, RD
0
0.5
1
1.5
2
2.5
1.0
0.6
0.2
DIMENSIØNLESS WATER

FIG. 3

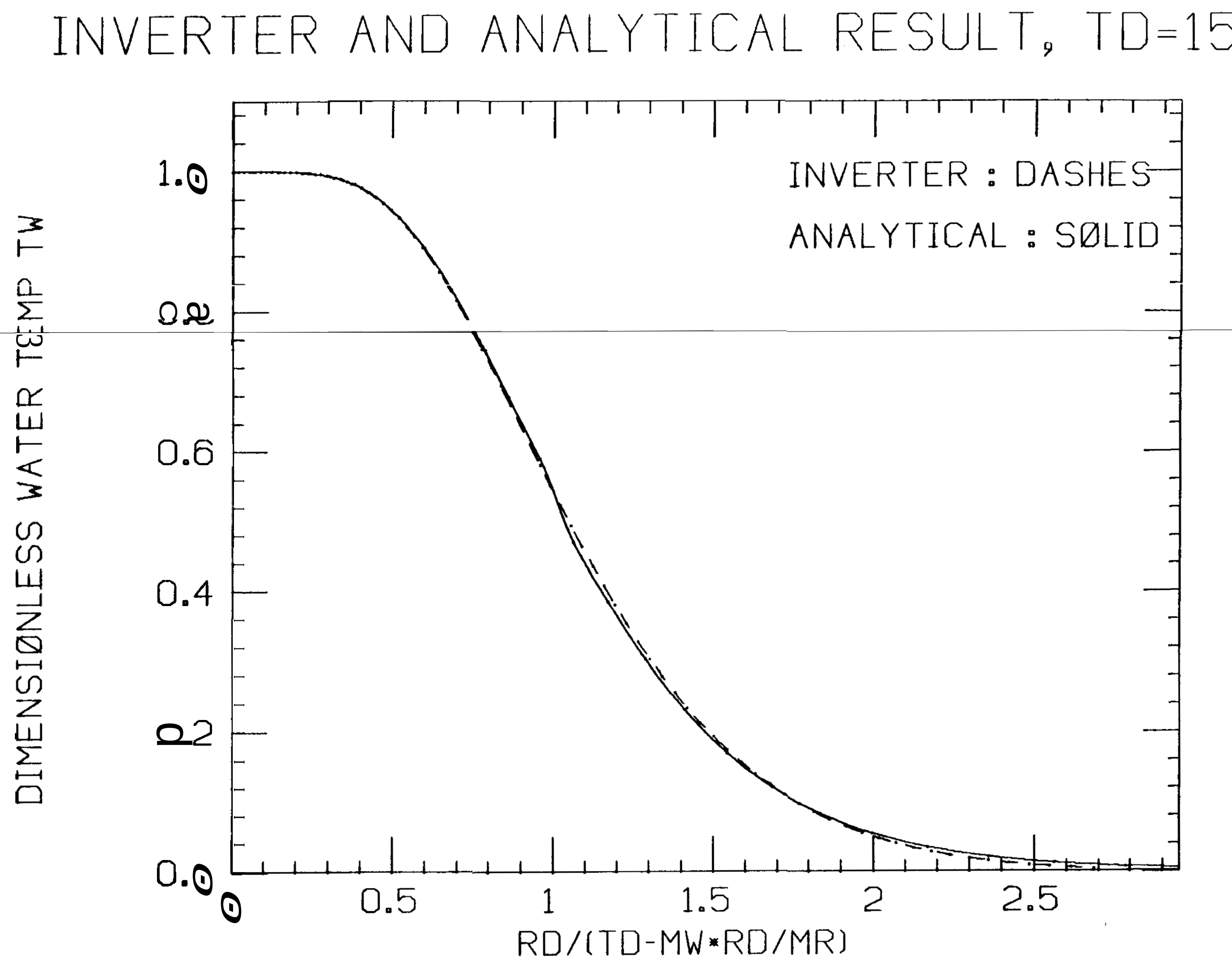
INVERTER AND ANALYTICAL RESULT, TD=15
INVERTER : DASHES
ANALYTICAL : SØLID
DIMENSIØNLESS WATER TEMP TW
RD/(TD-MW*RD/MR)
1.0
0.6
0.4
0.0
0
0.5
1
1.5
2
2.5

FIG. 4

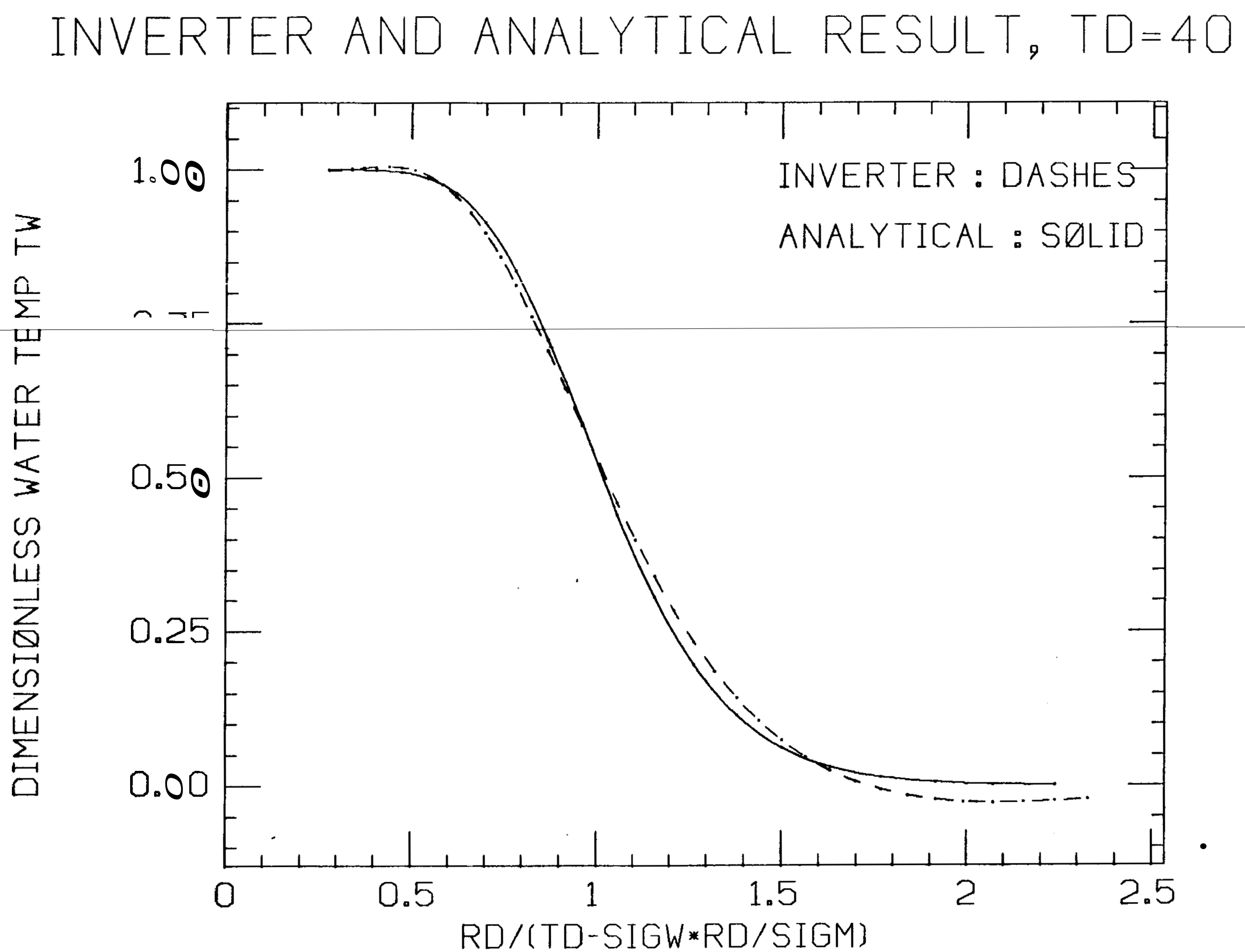
INVERTER AND ANALYTICAL RESULT, TD=40
INVERTER : DASHES
ANALYTICAL : SØLID
DIMENSIØNLESS WATER TEMP TW
1.00
0.50
0.25
0.00
0
0.5
1
1.5
2
2.5
RD/(TD-SIGW*RD/SIGM)

FIG. 5

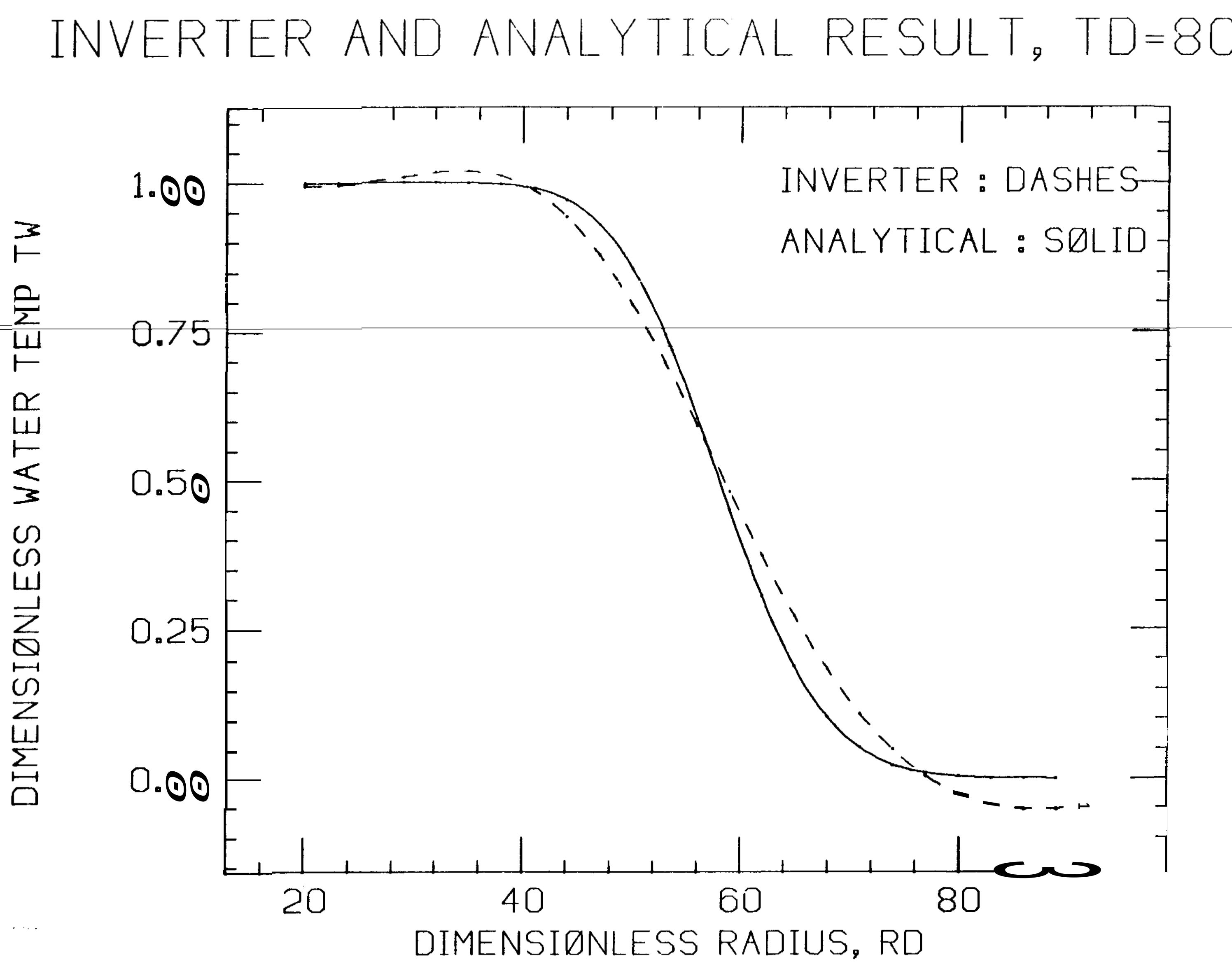
INVERTER AND ANALYTICAL RESULT, TD=80
INVERTER : DASHES
ANALYTICAL : SØLID
DIMENSIØNLESS WATER TEMP TW
1.00
0.75
0.50
0.25
0.00
20
40
60
80
DIMENSIØNLESS RADIUS, RD

FIG. 6

WOB 643 XJMJE214

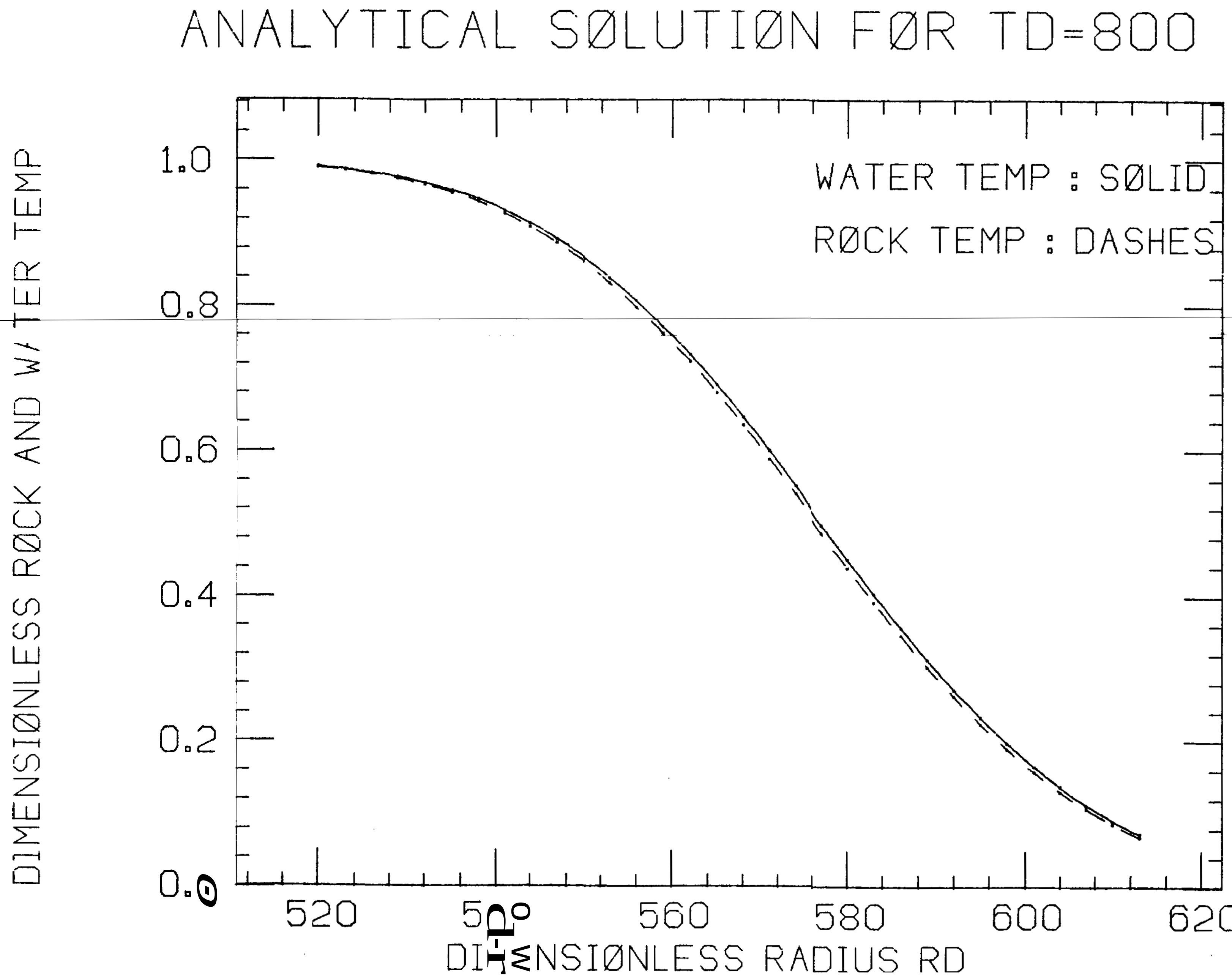

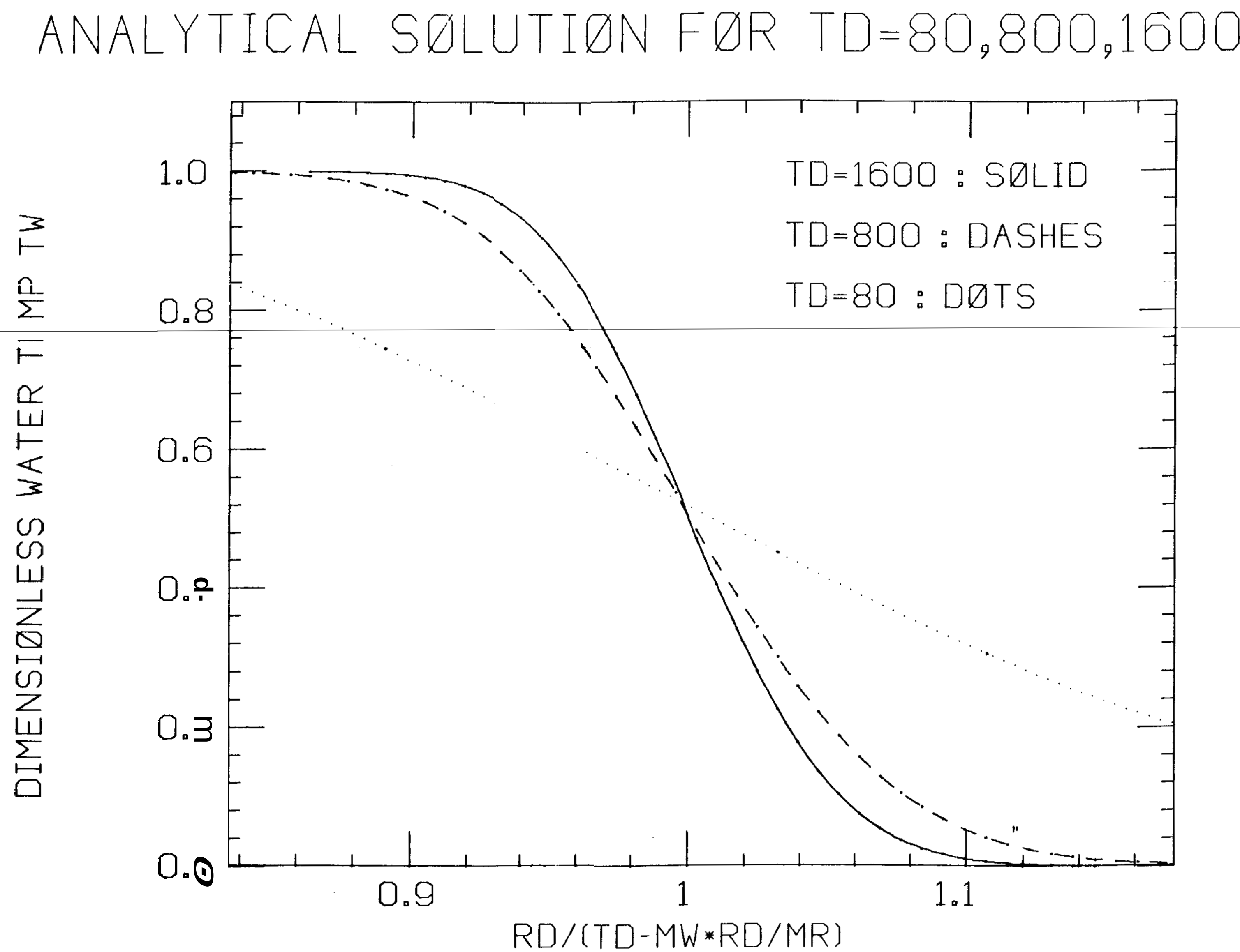
ANALYTICAL SØLUTIØN FØR TD=80,800,1600
TD=1600 : SØLID
TD=800 : DASHES
TD=80 : DØTS
DIMENSIØNLESS WATER TI MP TW
1.0
0.8
0.6
0.9
1
1.1
RD/(TD-MW*RD/MR)

FIG. 8

8 DISCUSSION OF ANALYTICAL RESULTS

The analytical results described are checked at the initial condition and boundary condition in Appendix 3. The asymptotic forms are also checked. For small times, equations (A3.2) and (A3.4) indicate an exponential form of solution, and Figures 2 and 3 show this effect. However, the numerical approximation of the modified Bessel function applies for only large values of x, and must be changed for smaller values. Furthermore, there exists a middle range where neither solution is well behaved. The Stehfest inverter is well behaved in this range, however, and it is used to match the analytical solution for the relatively small dimensionless time of 15[8]. At this value of dimensionless time, real time is about 6 minutes and the thermal front is developing from a simple step function through this exponential modification process. At a dimensionless time of 40 ,as shown in Fig. 5, the general symmetric form of the front is apparent and does not change until much later. Also, the Stehfest routine is shown to no longer match and is abandoned at this point. In Appendix 5, Figures 11 through 15 indicate the result using the inverter for later times.

Figures 5 through 9 are plots of the water and/or rock temperature for later times. These plots show that the front spreads as time increases but maintains its symmetric form. Figure 2 shows the relatively large difference in rock and water temperature at early dimensionless times. In Figures 9 through 11, this temperature difference is plotted at various times and is seen to decrease as time increases. For any given time, the maximum temperature difference occurs at the center of the front as expected. To the left of center, both the rock and water temperatures approach one (the injection temperature), while to the right of center, they approach zero (initial reservoir temperature). Equation (11) indicates that this plot is also that of the derivative of the rock temperature with respect to time, and that this has a maximum value at the center of the front, as one would expect. Further, these figures provide a simple measure of the spread of the front, as a rock-to-water temperature difference occurs only along the front.

9. FORM AND BEHAVIOUR OF THE THERMAL FRONT

The reason for the symmetry of the front can be seen from from equations (22) through (24). The upper portion of the curve is generated by case #1, which requires that the dimensionless radius to shifted-time ratio be less than or equal to one. At the center, r_D equals t_D and the dimensionless temperature equals 0.5. The lower portion of the curve is next generated by case #2 as r_D increases. If the dimensionless radius is divided by this ratio and plotted with dimensionless temperature, the center of the front is always located at one, for any dimensionless time. Figures 4 and 5 are two examples of this plot while Figure 8 plots the dimensionless water temperature for various times. From the latter plot it is seen that the curve steepens for larger times, indicating that the velocity of each point on the front approaches a constant value. This means that the rate of spread stops increasing and reaches a constant rate. This spreading change is also seen in Figs. 9, 10 and 11. For $t_D = 80$, approximately 95 % of the area is covered over a dimensionless distance of 60, while for $t_D = 800$, the distance is only 100, and for $t_D = 1600$, it is 200. The former implies an increasing rate of spread, while the latter two indicate a constant rate of spread.

For times significantly larger than those discussed above, the front does not behave in the same way. For a dimensionless time of 8000 and a constant velocity of each point on the front, one would expect a spread-distance of 1000. The actual value of this spread is about 350, much less than anticipated. Although the velocity of the center of the front (or average front velocity) does not change, the velocity of other points on the front must be decreasing. For times much larger, one might expect (given the results of Appendix 3), the following sequence of events :

(a). All points on the front approach the same velocity and the front no longer spreads.

(b). The front begins to shrink as the frontal velocities decrease at different rates.

(c) The front as such disappears and is replaced by the step function. The average radial velocity of the thermal front has now changed.

10. VELOCITY OF THE THERMAL FRONT

(i) Short and Intermediate Times

From plots such as Fig.11, one can determine the velocity of any point on the front since the location of the center of the front is fixed. Typical values of the plotted ratio $\frac{r_D}{t_D - \frac{M_w}{M_R} r_D}$ range from 0.5 to 1.5. Re-arranging this ratio, eliminating dimensionless terms, and differentiating with respect to time, gives the location and velocity of any point on the front for all but long times. The result for the short and intermediate times is :

$$q_w t = \pi\ (r^2 - r_w^2)\ \ell\ \left\{ \frac{\phi_R C_{vR}}{\phi_w C_{vw}} \frac{(1-\Phi_2)}{\eta} + \Phi_2 \right\} \qquad (32)$$

where,

$$\eta = \frac{r_D}{t_D} \qquad (33)$$

r is the radial distance to that point on the front, q_w is the flow rate of water injected into the reservoir, and $q_w t$ is the total reservoir volume of injected water.

Re-writing equation *(32)*, we have,

$$q_w t = \pi \left(r^2 - r_w^2 \right) \ell \zeta \tag{34}$$

where,

$$\zeta = \left\{ \frac{\rho_R C_{vR}}{\rho_w C_{vw}} \frac{(1-\Phi_2)}{\eta} + \Phi_2 \right\} \tag{34.1}$$

Differentiating *(32)* gives

$$\frac{q_w}{2\pi r \ell \Phi_2} = \frac{\zeta}{\Phi_2} \frac{\partial r}{\partial t} \tag{35}$$

Equation **(35)** can also be written in terms of radial velocities **as** :

$$V_h = \frac{\Phi_2}{\zeta} V_w \tag{36}$$

Where, V_h is the radial velocity of a given point on the thermal front, and V_W is the interstitial radial velocity of the water.

Note that for $\eta = 1$, equation *(32)* gives the location of the center of the thermal. front and equation *(34)* gives its velocity, which is also the average velocity of the front.

(ii) <u>Long Times</u>

For long times the front exists as the step function $u(t_D^*)$ and the above equations are replaced by :

$$q_w t = \pi (r^2 - r_w^2) \ell \Phi_2 \tag{37}$$

$$\frac{\partial r}{\partial t} = \frac{q_w}{2\pi r \ell \Phi_2} \tag{38}$$

or,

$$V_h = V_w \tag{38}$$

Equations (37) and (38) respectively correspond to equations (35) and (36) for $\zeta = \Phi_2$.

11. INTERPRETATION OF VELOCITY EQUATIONS

When the dimensionless terms are eliminated as shown above, the original energy balance relationships become clear. Dimensionless radius at the front becomes the total volume swept by that part of the thermal front, while the $q_w t$ term represents the total volume of injected fluid. Equations (32) and *(34)* also include the relative volumes of rock and water swept by the front, as the weighted sum of these terms is proportional to the total amount of injected heat. For large times, incremental volumes of injected water advance the thermal front by smaller increments of real radius or radial distance. In the limit, this increment of real radius is infinitesimally small and the thermal front must become step-like: with respect to the real radius. Eventually the front would also appear step-like with respect to the volume swept, as this convergence is proportional to r Ar . While this report does not examine plots of dimensionless temperatures versus real radius, this type of plot is easily made and clarifies the behaviour of the thermal front with respect the the real radial distance. It can also be used to estimate the times for using the velocity equations given above. In any case, the form and velocity of the front approaches that of the injected fluid.

JOB 5199 XJMJE196

ANALYTICAL SØLUTIØN CØNVECTIØN TERM

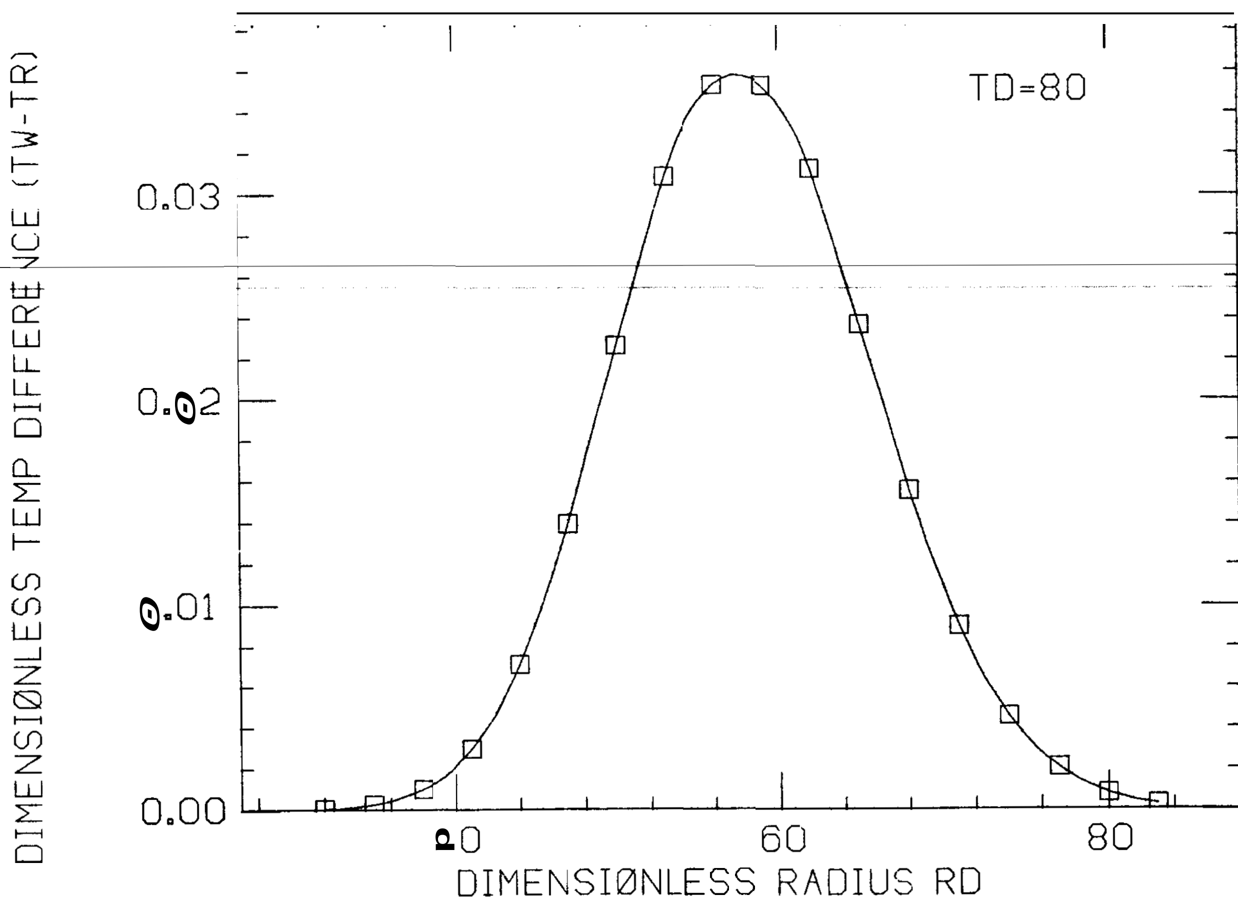

FIG. 9

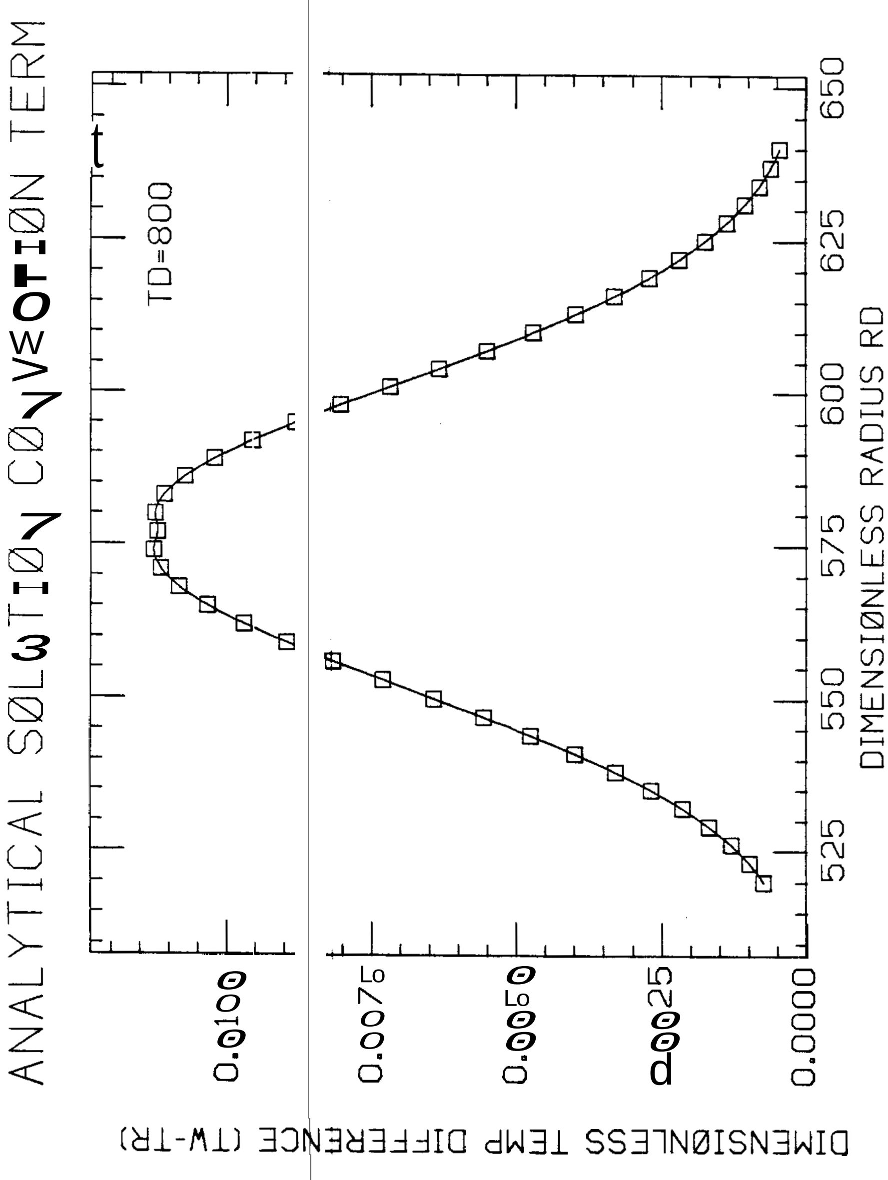
ANALYTICAL SØLUTIØN CØNVECTIØN TERM
TD=800
0.0100
0.0075
0.0050
0.0025
0.0000
DIMENSIØNLESS TEMP DIFFERENCE (TW-TR)
525
550
575
600
625
650
DIMENSIØNLESS RADIUS RD

FIG. 10

JOB 5139 XJMJE192

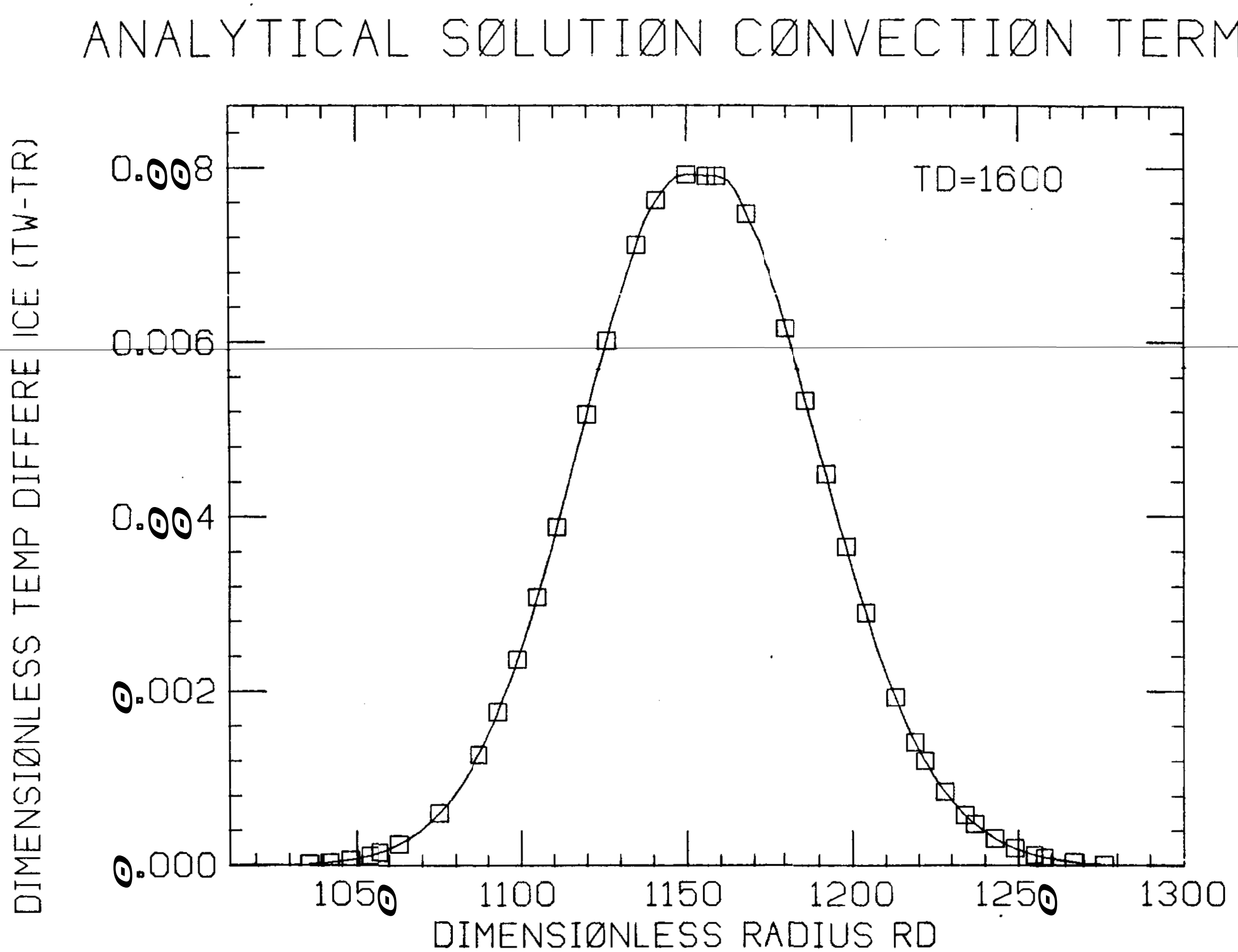

FIG. 11

12. CONCLUSIONS

Assuming one injection well in an infinite, naturally fractured geothermal reservoir, the results of this study apply for those times during which convection is the dominant form of heat transfer and fluid flow is steady state. The period therefore excludes very long and very short times.

Upon injection of water into the system, a thermal front of the form discussed quickly develops, and moves through the reservoir at a constant average rate. Its velocity is less than that of the injected fluid for relatively early time. Although at first the front spreads at an increasing rate, spreading gradually slows and eventually reverses itself. The rock and water temperature fronts become equal at a dimensionless time of about 1000 and move at the same rate thereafter. For times much greater than this, the front moves with the fluid, limited to step-like displacement of heat in the reservoir. As there is no conduction, the radial velocity of the thermal front decreases with the radial velocity of the fluid, and in the limit approaches zero.

As a final note, the problem presented in this report can be solved in a straightforward way using the Laplace transform. While numerical inversion routines are often of great value, analytical inversion appears to be the most reliable approach to a solution of this problem.

APPENDIX 1

Nomenclature		Typical Values
C_{vR}	Specific heat, rock, $\frac{btu}{lb\ ^\circ F}$	.228
C_{vw}	Specific heat, dater, $\frac{btu}{lb\ ^\circ F}$	1.00
ρ_R	**Density, rock,** $\frac{lb_m}{ft^3}$	170.00
ρ_w	Density, water, $\frac{lb_m}{ft^3}$	60.00
h_c	Convection constant, water, $\frac{btu}{hr\ ft^3\ ^\circ F}$	50.00
q_w	**Flow rate, water,** $\frac{ft^3}{hr}$	50.00
M_W	$\rho_w C_{vw} \Phi_2$, $\frac{btu}{ft^3\ ^\circ F}$	12.0
M_R	$\rho_R C_{vR}(1-\Phi_2)$, $\frac{btu}{ft^3\ ^\circ F}$	31.0
Φ_2	Fracture porosity, dimensionless	0.20
δ	Fracture width, ft	0.002

ℓ	Reservoir height, ft	25.00
r_w	Wellbore radius, ft	0.75
T_{wi}	Initial reservoir temperature, °F	400
T_{inj}	Temperature of injection fluid, °F	60
r_D	Dimensionless radius (actually a dimensionless volume term)	
t_D	Dimensionless time	
T_R , T_w	Dimensionless temperature of rock, water	
V_h , V_f	Radial velocity of heat, fluid, ft	

APPENDIX 2 : Laplace Space Solution

Transforming equations **(10)** and (11) implies :

$$- \frac{\partial \bar{T}_W}{\partial} - (\bar{T}_W - \bar{T}_R) = \frac{M_W}{M_R} s \, \bar{T}_W \qquad \text{(A 2.1)}$$

$$(\bar{T}_W - \bar{T}_R) = s \, \bar{T}_R \qquad \text{(A 2.2)}$$

Solving (A 2.2) for $\bar{T}_R$ and substituting it in (A 2.1) produces the following ordinary differential equation :

$$- \frac{\partial \bar{T}_W}{\partial_{\%}} - \left(1 + \frac{M_W}{M_R} \quad s \; \frac{1}{s+1}\right) \bar{T}_W = 0 \qquad \text{(A 2.3)}$$

Equation (13a) is derived by solving this ordinary differential equation for the water temperature and determining the constant of integration using the boundary condition. Equation (13b) is derived by substituting this result into equation (A 2.2).

APPENDIX 3 : Checks and Asymptotic Forms

Check of Initial and Boundary Conditions :

Initial Condition : $T_w(r_D,0) = T_R(r_D,0) = 0$ (12a)

Case # 2 applies for the initial condition above and from equations (24) and (25) it is seen that the step function ensures this for both the rock and water. As initially no heat (or cold) has been injected into the reservoir, one would expect the reservoir rock and water to be at their initial temperature.

Boundary Condition : $T_w(0,t_D) = 1$

(12b)

Case #1 applies for the above boundary condition, and it is easily seen from equation (23) that this condition is satisfied. Note, however, that the rock temperature should not satisfy this boundary condition, as it is dependent on the water temperature. This implicit condition is also satisfied.

Limiting Forms

Another useful che[illegible] for the analytical result is to examine the short and long time behaviour of the laplace space equation. The limiting forms of this equation are then inverted and compared with the analytical solution for [illegible]se times.

Short Time Solution

Water Temperature :

For short times, S [illegible] is large and equation (13a) approaches the form :

$$\overline{T}_w(r_D,S) = \mathrm{Exp}(-r_D)\,\frac{1}{S}\ \mathrm{I}\,[illegible]\,(-r_D\frac{M_w}{M_R}\,S) \qquad (A3.1)$$

After inverting,

$$T_w(r_D,t_D^*) = \mathrm{Exp}(-r_D)\ u[illegible] \qquad (A3.2)$$

Therefore one would exp[illegible] the short time solution for the water temperature to have an [illegible]nential form of front.

Rock Temperature Solution :

For large S, equation (13b) has the form :

$$\overline{T}_R(r_D,S) = Exp(-r_D)\,\frac{1}{S^2}\,Exp\left(-\,r_D\,\frac{M_w}{M_R}\,S\right) \tag{A3.3}$$

After inverting, this equation becomes :

$$T_R(r_D,t_D^*) = Exp(-r_D)\; t_D^*\; u(t_D^*) \tag{A3.4}$$

As $t_D \to 0$, $t_D^* \to 0$ and it is seen that the rock temperature approaches zero or is set to zero by the step function. The latter would be the case for all r_D if the time became zero as in the initial condition.

As another check, the asymptotic form of the inverted transform can be examined. The inverse transform of equation (13a) is equation (19.1).

$$T_R(r_D,t_D^*) = u(t_D^*)\,\{\,1 - J(t_D^*,r_D)\,\} \tag{19.1}$$

and the limiting forms are :

$$\lim_{y \to 0} J(x,y) = 1 \quad , \qquad \lim_{x \to 0} J(x,y) = Exp(-x) \tag{A3.5}$$

which is equivalent to :

$$\lim_{t_D^* \to 0} J(t_D^*, r_D) = 1 \quad , \quad \lim_{r_D \to 0} J(t_D^*, r_D) = Exp(-t_D^*) \tag{A3.6}$$

Substituting into (19.1), we have the same result for the rock temperature at short times.

If these limiting forms of the rock temperature for short time are also substituted into equation (A4.4), it is seen that as

$t_D^* \to 0$, $I_0(2\sqrt{r_D t_D^*}) \to 1$, and the water temperature

solution becomes :

$$T_w(r_D,t_D^*) = u(t_D^*)\ Exp(-r_D) \tag{A3.2}$$

which was obtained previously.

Long Time Solution

For long time, both the rock and water temperature solutions have the same form. For a given dimensionless radius (ie. volume), equations (13a) and (13b) approach the form :

$$\bar{T}_w(r_D,S) = \bar{T}_R(r_D,S) = \frac{1}{S} Exp(-r_D \frac{M_w}{M_R} S) \tag{A3.7}$$

After inverting, this equation becomes,

$$T_w(r_D,t_D^*) = T_R(r_D,t_D^*) = u(t_D^*) \tag{A3.8}$$

Therefore, one would expect the analytical solution to approach the form of the given step function for relatively long times.

Examining the inverted form of the solution again at the other limit :

$$\lim_{y \to \infty} J(x,y) = 1 \quad , \quad \lim_{x \to \infty} J(x,y) = 0 \tag{A3.9}$$

which is equivalent to,

$$\lim_{t_D \to \infty} J(t_D^*, r_D) = 0 \quad , \quad \lim_{r_D \to \infty} J(t_D^*, r_D) = 1 \tag{A3.10}$$

Substituting the first limiting form of (A3.10) into (19.1) gives the step function (A3.8). Substituting this result for the rock temperature into (19.2) gives the same result for the water temperature. Equation (A3.8) is the expected water and rock solution form for long time as both are equal and step functions.
The same results are also easily seen using case #1 of the expansion.

The same procedure can also be used to verify the analytical solution for large and small r_D.

APPENDIX 4 : Complete Derivation of Analytical Solution

Rock Temperature Solution :

The rock temperature solution for each case is found by substituting equations (20) or (21) into equation (19). The only other required substitution is allowing :

$$x = t_D^* \quad , \quad y = r_D \tag{A4.1}$$

After cancelling some terms, equations (22) and (24) are derived.

Water Temperature Solution :

$$T_w(r_D,S) = \frac{1}{S}\,\text{Exp}\left\{ - r_D\left(1 + \frac{M_w}{M_R} S - \frac{1}{S+1} \right) \right\} \tag{13a}$$

Re-writing equation (13a), as the sum of two parts,

$$T_w(r_D,t_D^*) = \text{Exp}\left(-r_D \frac{M_W}{M_R} S \right) \text{Exp}(-r_D)\left(\frac{1}{S+1}\,\text{Exp}\left(\frac{r_D}{S+1} \right) + \frac{1}{S(S+1)}\,\text{Exp}\left(\frac{r_D}{S+1} \right)\right) \tag{A4.2}$$

Inverting equation (A4.2) yields,

$$T_w(r_D,t_D^*) = u(t_D^*)\,\text{Exp}(-r_D)\,\mathcal{L}^{-1}\left\{ \frac{1}{S+1}\,\text{Exp}\left(\frac{r_D}{S+1} \right) \right\} + T_R(r_D,t_D^*) \tag{A4.3}$$

Using the same procedure outlined in equations (17) through (17.5), this becomes :

$$T_w(r_D,t_D^*) = u(t_D^*)\ \mathrm{Exp}\left\{ -\left(r_D + t_D^* \right) \right\} I_0\left(2\sqrt{r_D\ t_D^*} \right) + T_R(r_D,t_D^*) \tag{A4.4}$$

Substituting into (A4.4) the rock temperature solution for each case gives the water temperature solution for each case. Note that in both cases, the difference between the rock and water temperature solutions is the same function given in equation (26).

APPENDIX 3: Results of Numerical Inversion

This appendix contains the results obtained by inverting equations (13a) and (13b) numerically using the Stehfest routine.

For early dimensionless times up to *40*, a good match **of** the analytical solution is made. For times greater than this, however, the inverter is not well behaved and is not considered reliable. Figures 3 through 6 are plots of the numerical and analytical result for various dimensionless times. Note that the match is lost after *40* and worsens for later times. It appears that the match is lost when the Stehfest routine computes values of dimensionless temperature greater than one and less than zero. In addition, the thermal front as shown in Figures (12) through (16) would spread at increasing rates and never converge, a phenomenom which is physically impossible for this system. The Stehfest algorithm does prove useful however, for those early and mid-ranges **of** time during which the analytical solution is slowly convergent and/or the approximating equations (27a) and (27b) are not well behaved.

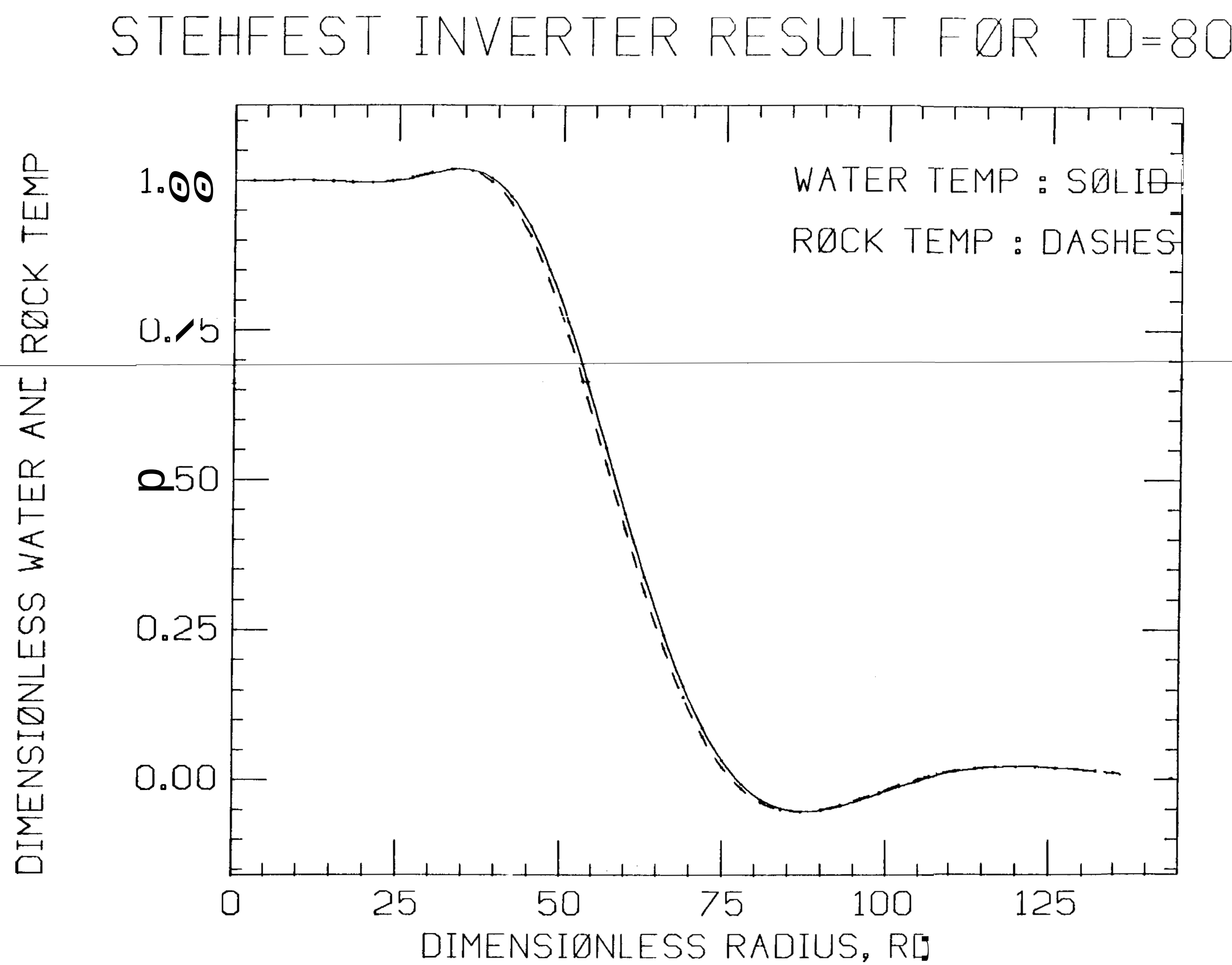
STEHFEST INVERTER RESULT FØR TD=80
WATER TEMP : SØLID
RØCK TEMP : DASHES
DIMENSIØNLESS WATER ANC RØCK TEMP
1.00
0.75
0.50
0.25
0.00
0
25
50
75
100
125
DIMENSIØNLESS RADIUS, RD

FIG. 12

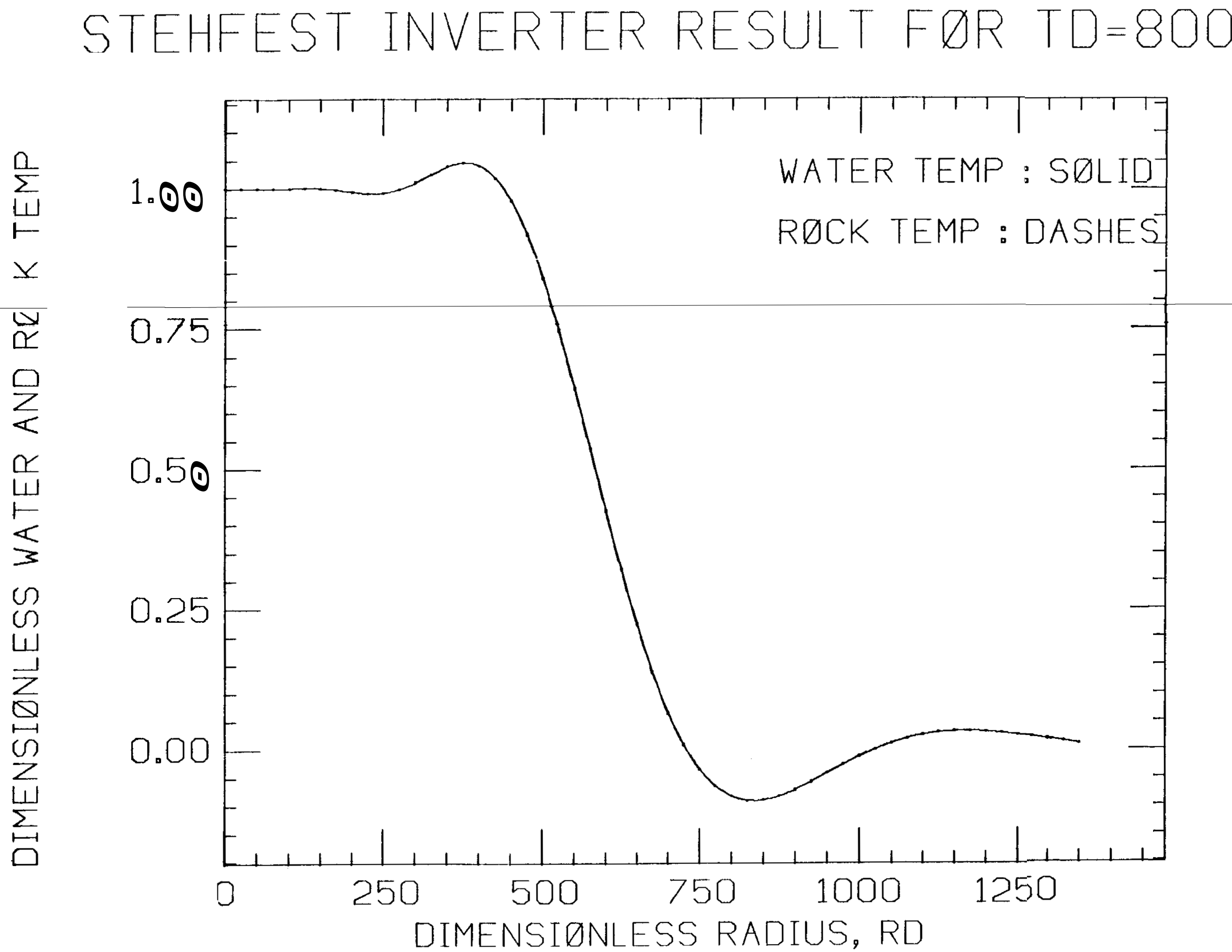
STEHFEST INVERTER RESULT FØR TD=800
WATER TEMP : SØLID
RØCK TEMP : DASHES
1.00
0.75
0.50
0.25
0.00
0
250
500
750
1000
1250
DIMENSIØNLESS RADIUS, RD
DIMENSIØNLESS WATER AND RØCK TEMP

FIG. 13

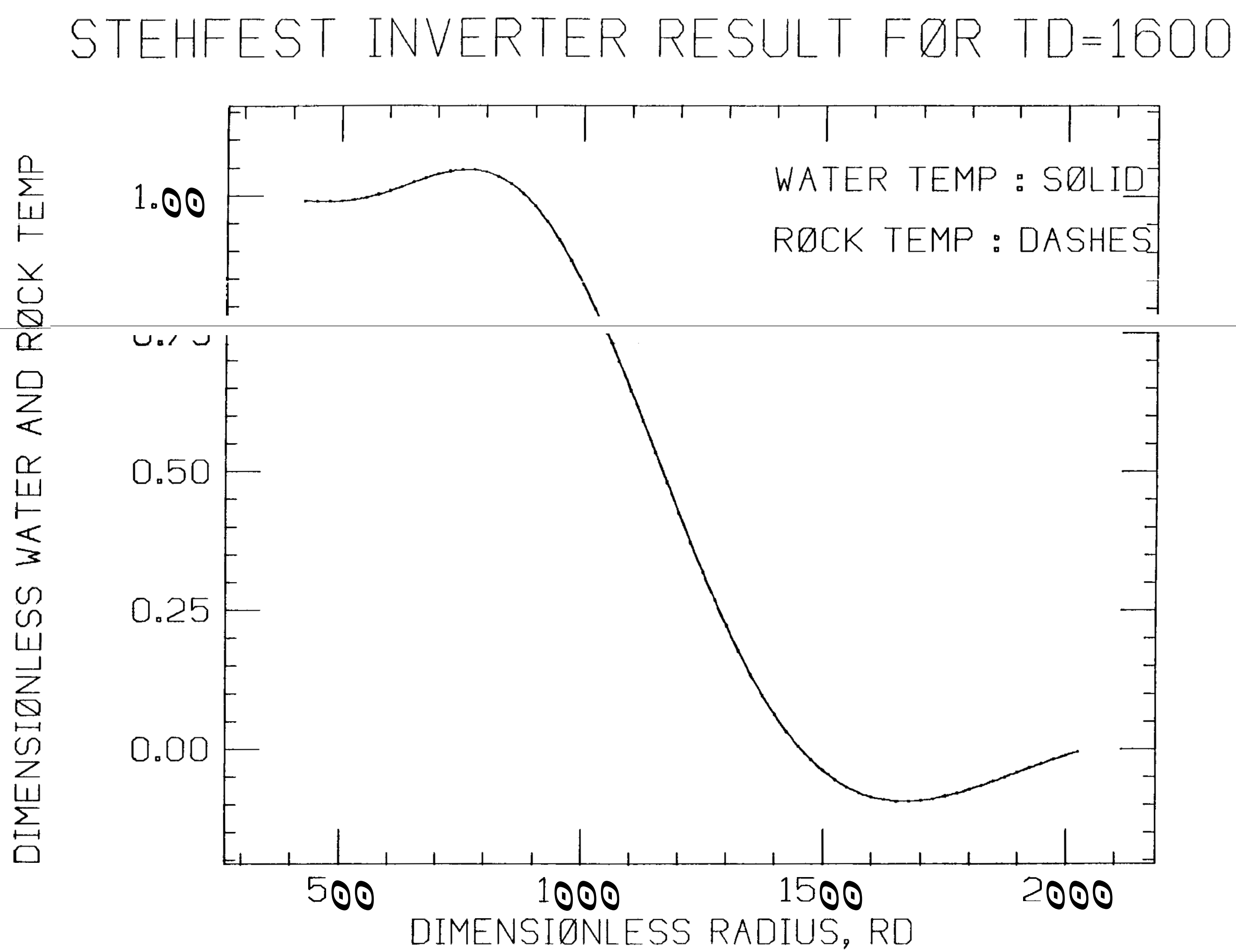

STEHFEST INVERTER RESULT FØR TD=1600
WATER TEMP : SØLID
RØCK TEMP : DASHES
1.00
0.50
0.25
0.00
DIMENSIØNLESS WATER AND RØCK TEMP
500
1000
1500
2000
DIMENSIØNLESS RADIUS, RD

FIG. 14

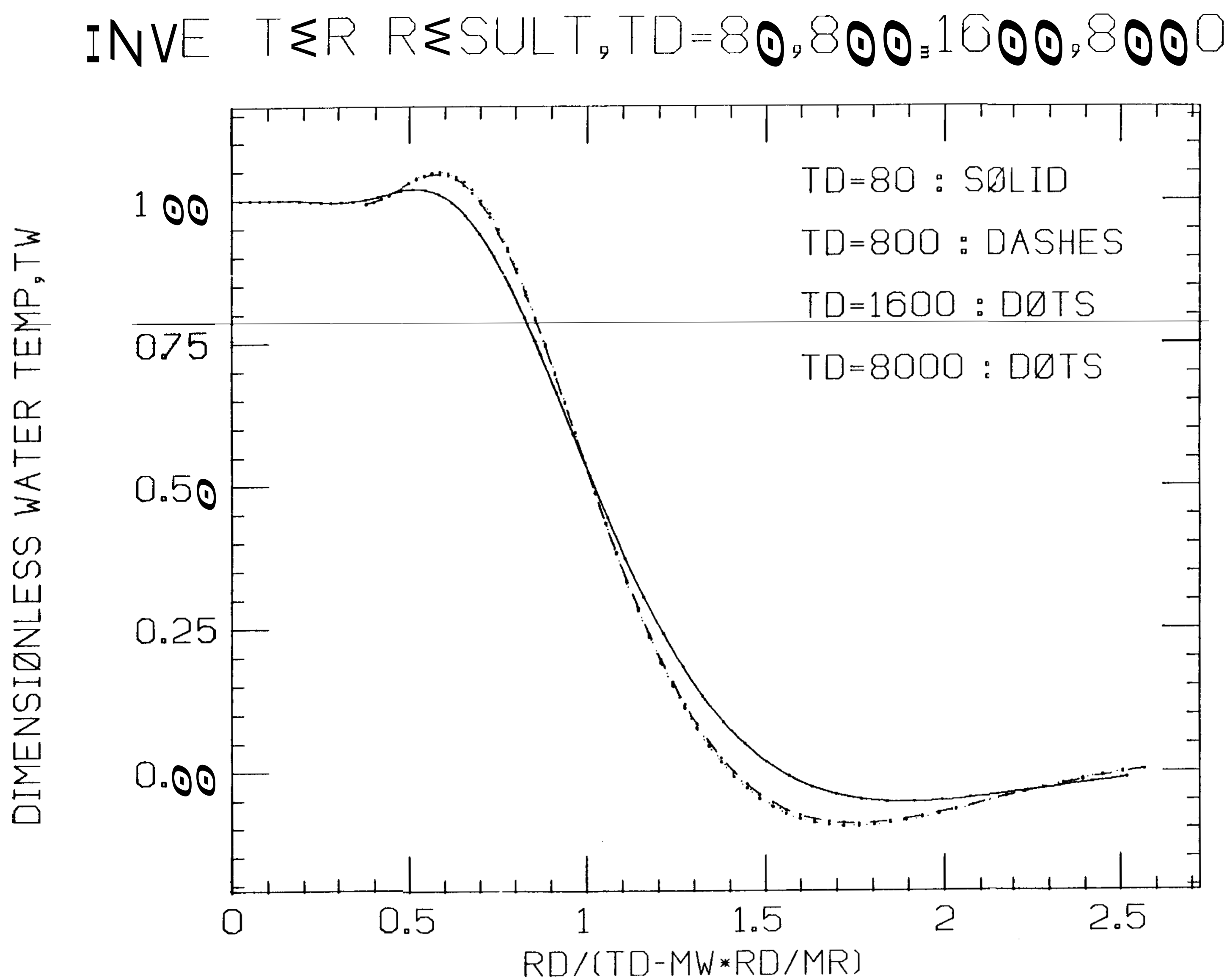
INVE T≷R R≷SULT,TD=80,800,1600,8000
TD=80 : SØLID
TD=800 : DASHES
TD=1600 : DØTS
TD=8000 : DØTS
1.00
0.75
0.50
0.25
0.00
DIMENSIØNLESS WATER TEMP,TW
0
0.5
1
1.5
2
2.5
RD/(TD-MW*RD/MR)

FIG. 15

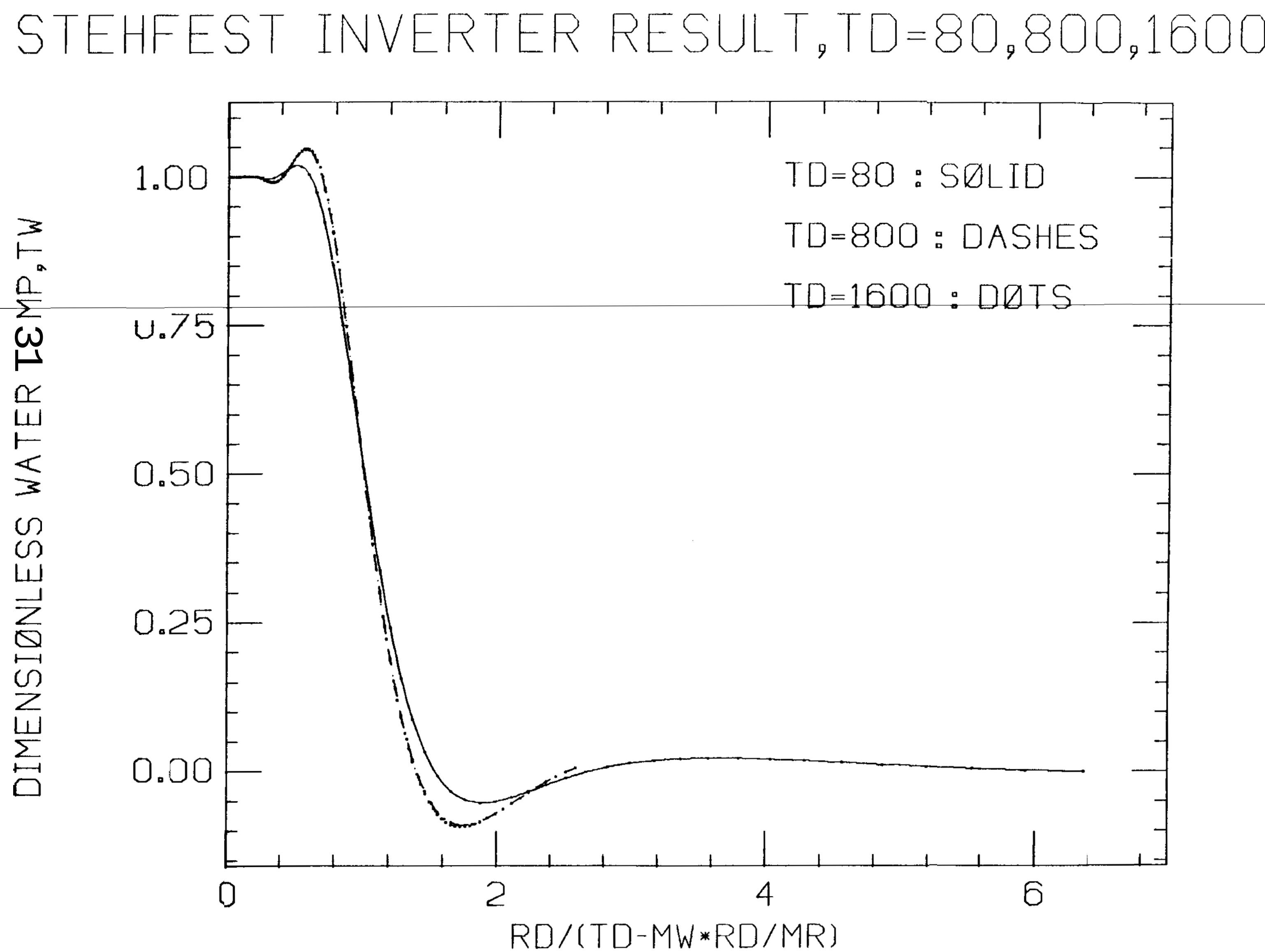
STEHFEST INVERTER RESULT,TD=80,800,1600
TD=80 : SØLID
TD=800 : DASHES
TD=1600 : DØTS
DIMENSIØNLESS WATER TEMP,TW
1.00
0.75
0.50
0.25
0.00
0
2
4
6
RD/(TD-MW*RD/MR)

FIG. 16

REFERENCES

1. Warren, J.E., and Root, P.J., 'The Behavior of Naturally Fractured Reservoirs', SPE Journal (Sept. 1963)

2. Mavor, Matthew J., 'Transient Pressure Behavior of Naturally Fractured Reservoirs', Master's Report, Department of Petroleum Engineering, Stanford University (1978).

3. Doetsch, 'Guide to the Application of Laplace Transforms', D. Von Nostrand, London, England; Toronto, Can.; New York, NY; Princeton, New Jersey (1961), pg.34.

4. Abramowitz and Stegun, 'Handbook of Mathematical Functions', Dover Publications, New York, NY (1970), pg. 1026.

5. Luke, 'Integrals of Bessel Functions', McGraw-Hill Book Co., New York, Toronto, London (1962), pgs. 271-283.

6. Op Cit, Luke, pg. 273,274.

7. Op Cit, Abramowitz and Stegun, pg. 375,377

8. Stehfest, H., 'Alogdrithm 368, Numerical Inversion of Laplace Transforms', D-5 Communications of the ACM (Jan. 1970)

BIBLIOGRAPHY

Davis, Harold T., 'The Summation of Series', The Principia Press of Trinity University, San Antonio, Texas (1962).

Doetsch, 'Guide to the Application of Laplace Transforms', D. Von Nostrand, London, England; Toronto, Can.; New York, NY; Princeton, New Jersey(1961).

Hansen, Eldon R., 'A Table of Series and Products', Prentice Hall, Inc. (1975).

Healy, Martin, 'Tables of Laplace, Heaviside, Fourier, and Z Transforms, W. and R. Chambers Ltd., Edinburgh and London(1967).

Kreith and Black, 'Basic Heat Transfer', Harper and Row Publishers, New York, NY(1980).

Kreyszig, Irwin, 'Advanced Engineering Mathematics', John Wiley and Sons Inc., New York, London, Toronto, Sydney (1972).

Weast, Astle, 'CRC Handbook of Chemistry and Physics', New York(1973).

```
// JOB
// EXEC WATFIV
      IMPL CIT REAL*8 (A-H,O-Z)
      COMM N TINJ,TWI,RW
      DOUB E PRECISION TD,RD,TUR,TUW
      QF=5 .0
      DENW 60.0
      CVW= .00
      HT=2 .00
      DENR 170.00
      CVR= .2280
      DELT 0.004
      HC=5 .00
      PHI2 0.20
      RW=0 750
      TWI= 30.00
      TINJ 50.00
C
C  ASSIGN ( INSTANTS
C
      B=DE J*QF*CVW/(2.0*3.1415927*HT)
      D=2.( *HC*PHI2/DELT
      SIGM )ENR*CVR*( 1.0-PHI21
      SIGW: )ENW*CVW*PHI 2
  250 FORM/ :(5X,3(3X,E18.11))
C
C  USE DIME (SIONLESS PARAMETERS
C
      TD=8( )0
      PRINT '  '
      PRINT '  '
C
      DO 9( LM=1,24
C
      RD=5( ID + 75*(LM-1)
      STEP1 :TD-SIGW*RD/SIGM
      IF(ST :P1.LT.0.0)GO TO 25
      CALL BES(STEP1,RD,1,TW1)
   25 IF(ST :P1.LT.0.0)TR1=0.0
      IF(ST :P1.LT.0.0)TW1=0.0
      PRINT '  '
      WRITE 6,250)RD,TW1
      PRINT '  '
C
   90 CONTI :UE
      STOP
      END
      SUBRO TINE IBES(TD,RD,I8,TE)
      IMPLI IT REAL*8 (A-H,O-Z)
      C3MMO  TINJ,TWI,RW
      DOUBL  PRECISION TE
C
C  THIS SUB OUTINE COMPUTES SUM OF BESSEL FNS I(Z)
C
      ADD=0 0
      Z=2.0 (RD*TD)**.5
      VX=(R /TD)**.5
C
      DO SO KK=1,235
      K=KK-
```

```
      IF(I8.EQ.1.AND.VX.LT.1.0)K=KK
      IF(I8.EQ.2.AND.VX.GT.1.0)K=KK
      U=4.0*K**2
C
      UPT=1.0
      FACJ=1
      SUMT=1.0
C
      DO 40 J=1,10
      FACJ=FACJ*J
      UPR=U-(2.0*J-1.0)**2.0
      UPT=-UPR*UPT
      TRM=UPT/(FACJ*(8.0*Z)**J)
      SUMT=SUMT+TRM
   40 CONTINUE
      KS=K
      IF(VX.GE.1)KS=-K
      VY=VX**KS
      BEI=VY*SUMT
      ADD=ADD+BEI
   80 CONTINUE
C
      CAN=Z-(TD+RD)
      IF(CAN.LT.-120.0)GO TO 82
      TE=(1.0/(2.*3.1415927*Z))**.5*DEXP(CAN)*ADD
   82 IF(CAN.LT.-120.0)TE=0.0
      IF(VX.LT.1.0)TE=1.0-TE
      RETURN
      END
$DATA
```

STEHFEST ROUTINE

```
// JOB
// EXEC WATFIV
      IMPLICIT REAL*8 (A-H,O-Z)
      EXTERNAL P
      COMMON G(50),V(50),H(25),GZ(1)
      COMMON TINJ,TWI,D,RW,RD,B,SIGM,SIGW
      DOUBLE PRECISION P
      M=1
      N=16
      QF=50.0
      DENW=60.0
      CVW=1.00
      HT=25.00
      DENR=170.00
      CVR=0.2280
      DELT=0.004
      HC=50.00
      PHI2=0.20
      RW=0.750
      TWI=400.00
      TINJ=60.00
C
C  ASSIGN CONSTANTS
C
      B=DENW*QF*CVW/(2.0*3.1415927*HT)
      D=2.0*HC*PHI2/DELT
      SIGM=DENR*CVR*(1.0-PHI2)
      SIGW=DENW*CVW*PHI2
C
  250 FORMAT(5X,3(3X,E19.10))
C
C  START LAPLACE INVERSION
C
      TD=15.0
C
      PRINT,' '
      PRINT,'  TD= ',TD
      PRINT,' '
C
      DO 20 LM=1,60
      RD=00.0+.50*(LM-1)
      PRINT,' '
      CALL LINV(P,TD,1,N,M,TAU1)
      CALL LINV(P,TD,2,N,M,TAU2)
      WRITE(6,250)RD,TAU1
   20 CONTINUE
      STOP
      END
      FUNCTION P(S,I7)
      IMPLICIT REAL*8 (A-H,O-Z)
      COMMON G(50),V(50),H(25),GZ(1)
      COMMON TINJ,TWI,D,RW,RD,B,SIGM,SIGW
      YY=1.0+SIGW*S/SIGM-1.0/(S+1.0)
      XY=S+1.0
      IF(RD*YY.GT.100.0)GO TO 91
      IF(I7.EQ.2)GO TO 90
      P=DEXP(-RD*YY)/S
      GO TO 92
   90 P=DEXP(-RD*YY)/(S*XY)
      GO TO 92
```